

# pHLIP-FIRE, a Cell Insertion-Triggered Fluorescent Probe for Imaging Tumors Demonstrates Targeted Cargo Delivery *In Vivo*

Alexander G. Karabadzhak,<sup>†</sup> Ming An,<sup>‡</sup> Lan Yao,<sup>§</sup> Rachel Langenbacher,<sup>‡</sup> Anna Moshnikova,<sup>||</sup> Ramona-Cosmina Adochite,<sup>||</sup> Oleg A. Andreev,<sup>||</sup> Yana K. Reshetnyak,<sup>||</sup> and Donald M. Engelman\*,<sup>†</sup>

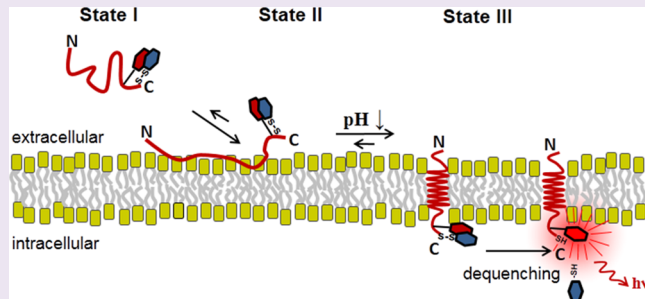
<sup>†</sup>Department of Molecular Biophysics and Biochemistry, Yale University, New Haven, Connecticut 06511, United States

<sup>‡</sup>Department of Chemistry and <sup>§</sup>Department of Physics, Applied Physics and Astronomy, State University of New York, Binghamton University, Binghamton, New York 13902, United States

<sup>||</sup>Department of Physics, University of Rhode Island, Kingston, Rhode Island 02881, United States

## S Supporting Information

**ABSTRACT:** We have developed an improved tool for imaging acidic tumors by reporting the insertion of a transmembrane helix: the pHLIP-Fluorescence Insertion REporter (pHLIP-FIRE). In acidic tissues, such as tumors, peptides in the pHLIP family insert as  $\alpha$ -helices across cell membranes. The cell-inserting end of the pHLIP-FIRE peptide has a fluorophore–fluorophore or fluorophore–quencher pair. A pair member is released by disulfide cleavage after insertion into the reducing environment inside a cell, resulting in dequenching of the probe. Thus, the fluorescence of the pHLIP-FIRE probe is enhanced upon cell-insertion in the targeted tissues but is suppressed elsewhere due to quenching. Targeting studies in mice bearing breast tumors show strong signaling by pHLIP-FIRE, with a contrast index of  $\sim 17$ , demonstrating (i) direct imaging of pHLIP insertion and (ii) cargo translocation *in vivo*. Imaging and targeted cargo delivery should each have clinical applications.



Imaging technologies are an important focus for improving the diagnosis of cancer and for guiding surgical and radiation therapies. Among the new tools, perhaps the greatest recent growth has come in the field of fluorescence imaging, with numerous new technologies now being adapted for clinical use.<sup>1,2</sup> One promising approach is the targeting of tumor biomarkers with fluorescent agents, allowing surgeons to visualize tumors in real-time during an operation. This advance has the potential to improve the success of surgical interventions by giving an active real-time marker of tumor borders, which are often hard to distinguish from the surrounding healthy tissue.<sup>3</sup> The primary goal in imaging-agent design is a high target-to-background ratio: agents should contribute minimal background but have high local concentrations at intended target sites. The “self” nature of targeted markers often leads to background signals too high for effective discrimination of tumors. A further complication lies in the diverse nature of human cancers. Since heterogeneous marker expression is often found within regions of a tumor, and further since no two cancers are identical, it is unlikely that a single marker can be relied upon.<sup>4</sup>

As an alternative to biomarker targeting, we have suggested that the acidic environment within solid tumors may be exploited for targeting by the pH (Low) Insertion Peptide (pHLIP) family.<sup>5</sup> Malignant tumors exhibit elevated uptake and consumption of glucose, as well as metabolite buildup and hypoxia due to inadequate blood supply, leading to tumor

acidosis from the Pasteur and Warburg effects.<sup>6–8</sup> As a result, the extracellular environment in virtually all solid tumors is acidic ( $\text{pH} \sim 6.0\text{--}6.5$ ),<sup>9,10</sup> and more aggressive tumors are more acidic.<sup>11</sup> Extracellular acidity may therefore be a general biomarker for targeting malignant tumors.

The original pHLIP is a 36-amino-acid peptide, and a number of versions with different properties have now been found that constitute the family of pHLIPs.<sup>5</sup> A pHLIP exists as a soluble, unstructured monomer with an affinity for cell membranes at physiological pH. The adsorption to a model POPC membrane at high pH is accompanied by the release of about  $5\text{--}7 \text{ kcal mol}^{-1}$  of energy.<sup>5,12</sup> At low pH ( $\text{pH} \leq \sim 6$ ), pHLIP folds to form a transmembrane  $\alpha$ -helix, inserting its C-terminus across the cell membrane. The transition proceeds with an additional release of  $1.5\text{--}2 \text{ kcal mol}^{-1}$  of energy. This pH-dependent insertion is triggered by protonation of carboxyl groups on residues in the peptide transmembrane region and peptide inserting end. The protonation effectively increases the overall hydrophobicity of pHLIP, permitting the insertion.<sup>13</sup> Serendipitously, the extracellular pH at which pHLIP undergoes its insertion transition corresponds closely to the extracellular pH produced in acidic solid tumors. Using

Received: May 16, 2014

Accepted: September 3, 2014

Published: September 3, 2014

peptides covalently modified with fluorescent dyes at the noninserting N-terminus, pHILIP has been shown to target both spontaneous and implanted tumors in small animal models, although slow background clearance has limited the contrast ratios that can be attained.<sup>14–18</sup> The insertion energy can be used to deliver cargo molecules into cells, by biasing the equilibrium between surface and inserted forms in favor of the transport of cell-impermeable polar molecules attached to the C-terminus.<sup>19–21</sup> While such delivery has been explored in cells, the step of demonstrating cytoplasmic delivery in tumors in an animal had not been taken before the work we report here.

To improve contrast and to document transmembrane insertion delivery *in vivo*, we have developed the pHILIP Fluorescence Insertion REporter system (pHILIP-FIRE), with the main goal as enhancing fluorescent signal upon insertion into cells in diseased tissue. pHILIP-FIRE peptides possess neighboring lysine and cysteine residues in the cell-inserting, C-terminal end. The lysine side-chain is irreversibly covalently linked to a fluorophore via an amide bond. The neighboring cysteine side-chain is covalently linked by a disulfide bond to a fluorescence quencher or another fluorophore (for self-quenching). When these moieties are both present on the peptide, the fluorescence is quenched, but upon insertion of the C-terminus into the reducing environment of a living cell, the quenching moiety is released by disulfide reduction, leading to the dequenching of the fluorophore emission (Figure 1). The

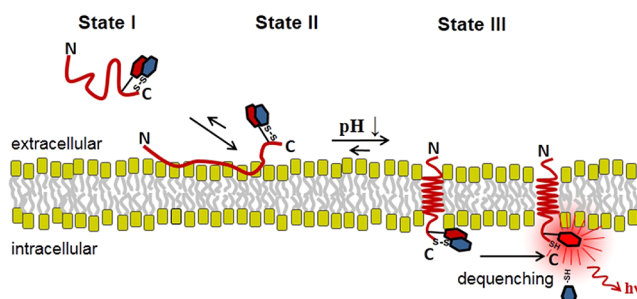


**Figure 1.** Activation of pHILIP-FIRE. State I: the peptide is soluble and unstructured in aqueous solution at physiological pH. State II: The peptide binds to the surface of a cell membrane in an unstructured form at physiological pH. State III: At acidic pH, the peptide forms an  $\alpha$ -helix and inserts across the membrane, placing the self-quenching dye construct in the reducing environment of the cytoplasm. The fluorescence of the dye is activated by disulfide cleavage that disrupts the fluorophore/quencher pair, dequenching the construct and producing strong fluorescence.

pHILIP-FIRE strategy aims to increase the contrast of fluorescence imaging *in vivo* by quenching background signals. We report tumor imaging with improved sensitivity, as well as demonstrating for the first time pHILIP insertion and cargo delivery *in vivo*.

## RESULTS AND DISCUSSION

Our strategy of pHILIP-FIRE is based on fluorescence quenching, which occurs upon close proximity of either two fluorophores (homoquenching and H-dimer formation) or a fluorophore-quencher pair (heteroquenching). When one of the members of a pair is released, in our case by disulfide cleavage in the cytoplasm, the result is greatly enhanced observable fluorescence. Accordingly, we designed and synthesized two pHILIP-FIRE constructs. The first construct, pHILIP-T-T, carries two TAMRA fluorophores that are self-

quenched by forming an H-dimer, with one attached to pHILIP via a disulfide bond. The second construct, pHILIP-T-Q, has a TAMRA-QSY9 pair, where the quencher (QSY9) is attached to pHILIP via a disulfide bond. To control for quenching activity, a pHILIP with a single, unquenched TAMRA dye covalently linked to a C-terminal cysteine via a thioether bond was also synthesized and tested. The constructs used in this study are as follows:

**pHILIP-T-T:** AAEQNPIYWARYADWLFTTPLLL DLLVDAEGTK(TAMRA)C(TAMRA)G

**pHILIP-T-Q:** AAEQNPIYWARYADWLFTTPLLL DLLVDAEGTK(TAMRA)C(QSY9)G

**pHILIP-T:** AAEQNPIYWARYADWLFTTPLLL DLLVDAEGTC(TAMRA)

**Chemical Fluorescence Dequenching.** The spectral properties of each pHILIP-FIRE construct were investigated in solution in the absence and presence of a reducing agent. Glutathione (GSH) is the primary reducing agent in living cells, with an intracellular concentration of up to 10 mM, depending upon the intracellular compartment and the cell cycle.<sup>22</sup> We used 1, 3, or 10 mM concentrations of glutathione to simulate reductive and physiologically reasonable intracellular conditions. pHILIP-FIRE dequenching was observed by absorbance and fluorescence spectroscopy. The absorbance peak of the TAMRA–TAMRA H-type dimer (in pHILIP-T-T) is blue-shifted to 524 nm from the usual monomer TAMRA absorbance maximum at 555 nm.<sup>23</sup> The blue-shifted TAMRA–TAMRA dimer absorbance peak was replaced by an augmented 555 nm TAMRA peak following disulfide reduction in the pHILIP-T-T peptide with 10 mM glutathione. As expected, in contrast to pHILIP-T-T, the shape of the absorbance spectrum of pHILIP-T-Q does not change significantly after the cleavage of the S–S bond and resulting quencher separation (Figure 2a). The activation of the pHILIP-T-Q and pHILIP-T-T probes were each monitored by changes in the TAMRA fluorescence signal. After incubation with 10 mM glutathione, the pHILIP-T-Q or pHILIP-T-T fluorescence was excited at 555 nm, and emission was followed at its 580 nm maximum (Figure 2b). An increase in emission intensity was observed over time following the addition of glutathione (1, 3, or 10 mM). Fluorescence intensity was plotted as a function of time and fit using a single exponential function (Figure 2d). The fluorescence of each pHILIP-FIRE construct was significantly quenched when compared to the emission of pHILIP-T (Figure 2c). The addition of glutathione did not alter the fluorescence intensity of pHILIP-T, whereas a 7 to 18-fold increase in fluorescence intensity was observed for the pHILIP-FIRE constructs after 3 h. Our data show the expected higher dequenching signal for pHILIP-T-T compared to pHILIP-T-Q, since two moles of TAMRA are dequenched in the T-T case. The kinetics of activation depend on the glutathione concentration: At 10 mM GSH, the rates are  $k = 4.7 \text{ h}^{-1}$  and  $3.4 \text{ h}^{-1}$  for pHILIP-T-T and pHILIP-T-Q respectively, whereas at 1 mM GSH, the rates are  $k = 1.1 \text{ h}^{-1}$  and  $0.4 \text{ h}^{-1}$  (Supporting Information Table 1).

The pH-dependent interactions of pHILIP-FIRE peptides with artificial membranes were followed by circular dichroism (CD). Peptides were incubated with 100 nm POPC liposomes overnight in pH 8 phosphate buffer and the pH was dropped rapidly to pH 4 by the addition of concentrated HCl. When measured alone in solution or in the presence of liposomes at pH 8, pHILIP-FIRE exhibited CD spectra characteristic of an unstructured peptide, with a negative ellipticity peak around

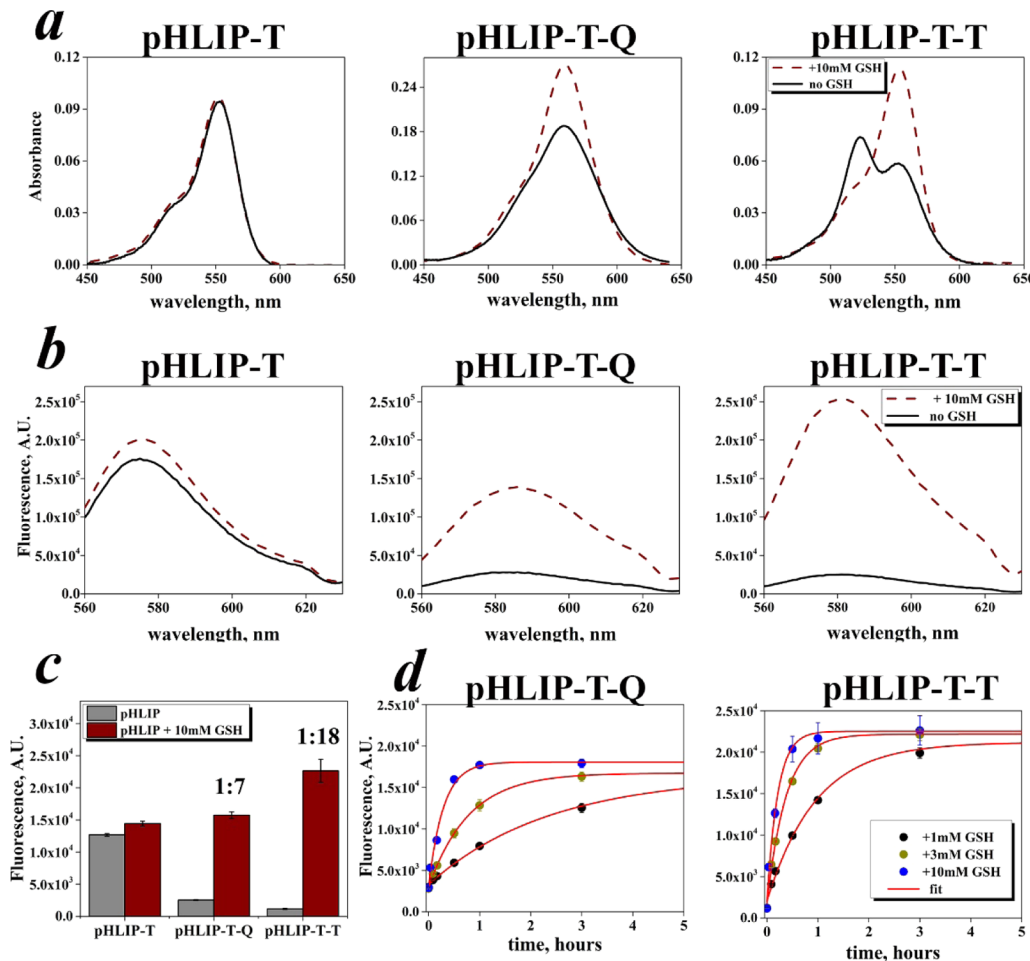


**Figure 2.** Chemical dequenching of pHLIP-FIRE constructs. (a) Absorbance spectra of  $1\ \mu\text{M}$  pHLIP-T, pHLIP-T-Q, and pHLIP-T-T before (solid line) and after (dashed line) treatment with  $10\ \text{mM}$  of glutathione. The red-shifted peak (dashed line) of the reduced pHLIP-T-T construct results from the conversion of H-dimer to monomeric TAMRA. (b) Fluorescence spectra of  $1\ \mu\text{M}$  pHLIP-T, pHLIP-T-Q, and pHLIP-T-T before (solid line) and after (dashed line) treatment with  $10\ \text{mM}$  of glutathione. (c) TAMRA fluorescence level and dequenching capacity of quenched pHLIP-T-Q and pHLIP-T-T constructs ( $1\ \mu\text{M}$ ) and the nonquenched control pHLIP-T ( $1\ \mu\text{M}$ ) before (gray bars) and after (red bars) the addition of  $10\ \text{mM}$  glutathione. (d) Time-course of dequenching of pHLIP-T-Q or pHLIP-T-T ( $1\ \mu\text{M}$ ) after the addition of  $1$ ,  $3$ , or  $10\ \text{mM}$  of glutathione. The dequenching rates are presented in Supporting Information Table 1. Error bars, standard deviation (SD) ( $n = 3$  experiments).

200 nm. When the pH was dropped to 4, a characteristic CD  $\alpha$ -helical signal was observed, with two negative ellipticity peaks at 208 and 222 nm and a positive peak at 195 nm. The CD data show that the pHLIP-FIRE constructs exhibit the three states of pH-dependent membrane insertion characteristic of pHLIP peptides (Figure 3).

**pHLIP-FIRE Activation in Cultured Cells.** pH-triggered activation of each pHLIP-FIRE probe was tested in cultured cells grown at normal pH medium (HeLa and COS-7) or adapted for low pH growth (AS49). HeLa and COS-7 cells were incubated with pHLIP-FIRE peptides ( $1\ \mu\text{M}$ ) for 20 min at room temperature (RT) ( $\sim 22\ ^\circ\text{C}$ ) either at pH 7.4 or at pH 6.1 DPBS buffer in 96-well plates. Cells were then washed three times with DPBS buffer (pH 7.4 or pH 6.1) and DMEM (pH 7.4 or pH 6.1) was added before measurements were performed at each experimental pH. TAMRA fluorescence was measured immediately after washing (time zero used for normalization), then at multiple time points for up to 2 days following the incubation and wash steps. TAMRA fluorescence intensity steadily increased over 2 days following incubation at low pH conditions to a maximum intensity of 16-fold over the zero time point. Higher TAMRA fluorescence signals (8–16

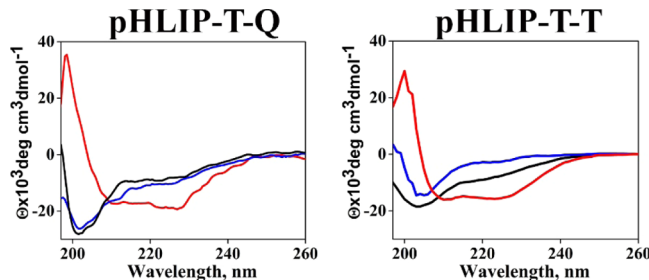


**Figure 3.** Peptide conformations in the three states of the pHLIP-FIRE constructs. The pHLIP-T-Q and pHLIP-T-T CD spectra. The pHLIP-FIRE peptides were studied for the presence of the three basic states of pHLIP: state I is the peptide in solution at pH 8 (black line), state II is the peptide in the presence of POPC liposomes at pH 8 (blue line), and state III is the folding and insertion of the peptide with POPC when the pH is dropped from pH 8 to pH 3.7 by the addition of an aliquot of HCl (red line). The inserted state is monitored by changes of the CD spectral signal. The concentrations of pHLIP constructs and POPC were  $4\ \mu\text{M}$  and  $0.8\ \text{mM}$ , respectively.

fold increase) were observed in cells (HeLa and COS-7) incubated with pHLIP-FIRE peptides at pH 6.1 as compared to

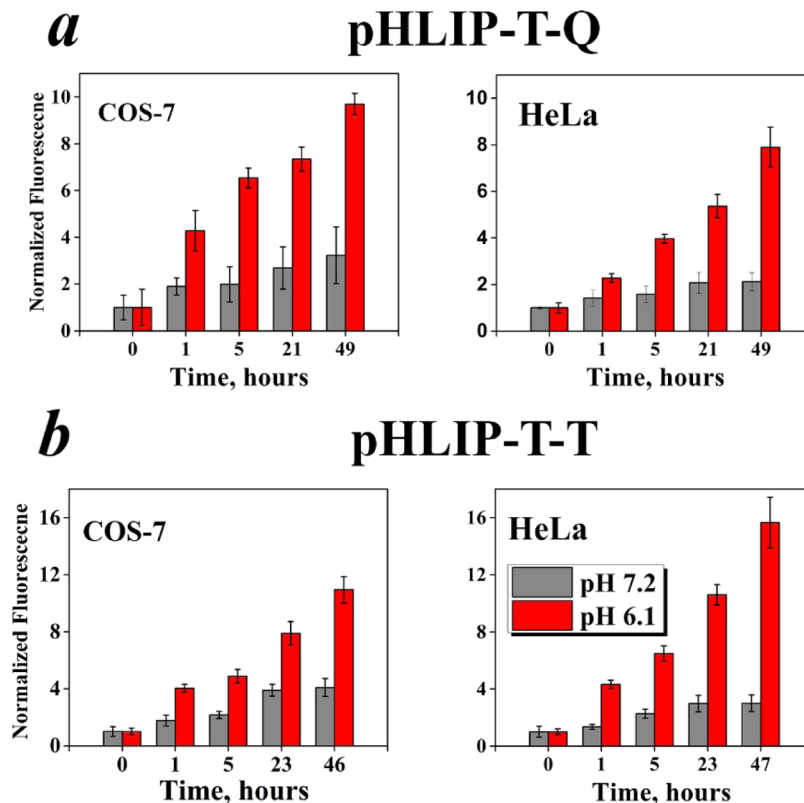


**Figure 4.** Changes of fluorescence intensity of TAMRA upon insertion. Insertion of pHЛИP-T-Q (a) and pHЛИP-T-T (b) into HeLa and COS-7 cells at pH 6.1 (red bars) and pH 7.4 (gray bars) at different time points are shown. Dequenching of the fluorophore is facilitated by the highly reducing environment inside the cells. All signals are normalized to the intensity at time zero. Error bars, SD ( $n = 6$  experiments).

the fluorescence increase following incubation and washing at pH 7.4 (2–4 fold increase) (Figure 4). Activation of the pHЛИP-FIRE at neutral pH might occur due to (i) membrane insertion of some amount of the construct at pH 7.2–7.4, since there is an equilibrium between inserted and surface locations of the peptide, or (ii) endocytotic uptake of the peptide adsorbed at the membrane surface, especially since the time course of the experiment is several days, or both. The fluorescence data were fitted with a single exponential nonlinear regression. For constructs at low pH the rate constants were found to be  $\sim 0.8$ – $1.38 \text{ h}^{-1}$  with a positive linear slope of 0.08–0.23 (Figure 5), similar to rates observed in the chemical dequenching experiments with glutathione concentrations from 1–3 mM (Supporting Information Table 1). The linear component of the fitting signal may arise from a second population of pHЛИP-FIRE, in which some other mechanism is involved, such as nonspecific endocytotic uptake of the constructs, producing slow kinetics. Interestingly, the linear component of nonspecific uptake is higher for HeLa cells than COS-7 cells, possibly indicating that different cell types internalize the peptide via different pathways and at different rates.

The A549 cells adapted to low pH growth were incubated with pHЛИP-FIRE peptides (1  $\mu\text{M}$ ) or the unquenched control peptide, pHЛИP-T (1  $\mu\text{M}$ ), for 20 min as described above, then washed cells were kept in culture at pH 6.1. Fluorescence was measured at intervals for 4 days after treatment. pHЛИP-T showed no significant change in fluorescence (2-fold background increase) over the course of these measurements, whereas both pHЛИP-T-T and pHЛИP-T-Q showed an 8- to 10-fold increase in fluorescence at 74 h after incubation (Figure 6).

By itself, pHЛИP shows no signs of toxicity in cells or animals.<sup>5,21</sup>

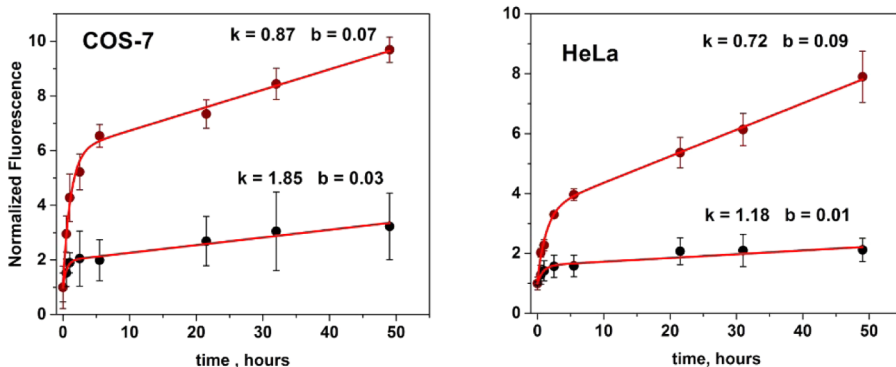
#### Confocal Microscopy of pHЛИP-T-T Activation in Cells.

We used confocal microscopy to visualize pH-dependent TAMRA release and distribution inside cultured cells. The cells were treated with 1  $\mu\text{M}$  of pHЛИP-T-T as described above. Thirty minutes before imaging, the cells were treated with Hoechst to stain the nuclei. When C-terminus of the construct is inside the cytoplasm we expect to see TAMRA fluorescence signal throughout the cytoplasm due to release of the disulfide linked TAMRA. Confocal microscopy shows that this is the case at pH 6.1 but not at pH 7.4. Interestingly, we observed some “punctate” fluorescence at pH 7.4, which might be attributed to endocytic uptake of the construct by HeLa (Figure 7).

**Imaging In Vivo.** Because of their pH-dependent interaction with membranes, pHЛИP peptides have been shown to target and persistently label cells in acidic tissues, such as cancerous tumors, *in vivo*.<sup>24,25</sup> pHЛИP peptides have also been successfully used to translocate cell-impermeable molecules across the membranes of cultured cells in a pH-dependent manner.<sup>19,20</sup> Here, we take the next step: demonstrating targeted delivery into tumor cells *in vivo*.

Balb/c mice bearing implanted 4T1 murine breast tumors were used to assess the tumor targeting and biodistribution properties of pHЛИP-FIRE in comparison with pHЛИP-T. Mouse tumors were established by subcutaneous injection of 4T1 cells ( $8 \times 10^5$  cells) in the right flank of each mouse. When tumors reached 5 to 6 mm in diameter, each of the pHЛИP-FIRE peptides and the unquenched control pHЛИP-T were given as single injections into the tail veins of groups of mice.

## pHLIP-T-Q



## pHLIP-T-T

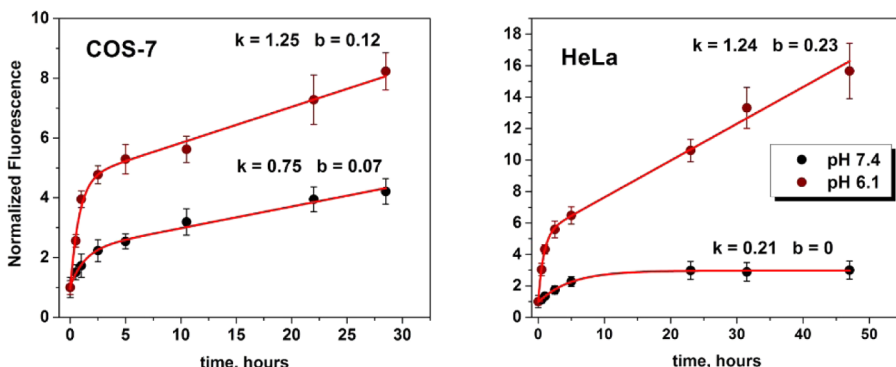


**Figure 5.** Kinetics of dequenching of pHLIP-FIRE fluorescence resulting from cell insertion. All data points were fitted using a single exponential function with a sloped asymptotic line  $y = A \cdot \exp(-kt) + bx + y_0$ . Error bars, SD ( $n = 6$  experiments).

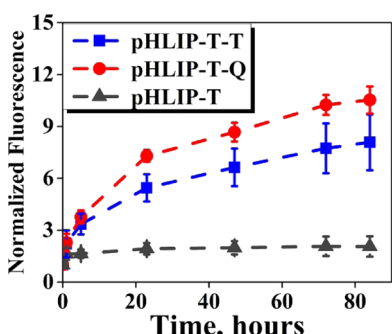


**Figure 6.** Incubation of pHLIP-FIRE with A549 cells at pH 6.1. Normalized TAMRA fluorescence intensities of pHLIP-T (black triangle), pHLIP-T-Q (red circle), and pHLIP-T-T (blue square). The pHLIP-T control (not quenched) showed a 2-fold increase in fluorescence. This 2-fold background increase may be due to the partial shielding effect of insertion into the cell or due to the different environmental conditions inside vs outside of the cells. Error bars, SD ( $n = 5$  experiments).

Peptides were injected at  $\sim 1$  mg/kg, with adjustments made to deliver equimolar dosages of the varied peptide constructs. Animals were euthanized at 24 or 48 h following injection, and necropsy was performed immediately thereafter. Tumors and major organs were excised and imaged on an FX Kodak *in vivo* image station. Imaging was performed for each animal using a uniform set of illumination and exposure parameters in order to allow accurate comparison of the resulting intensities (Figure 8a, b).

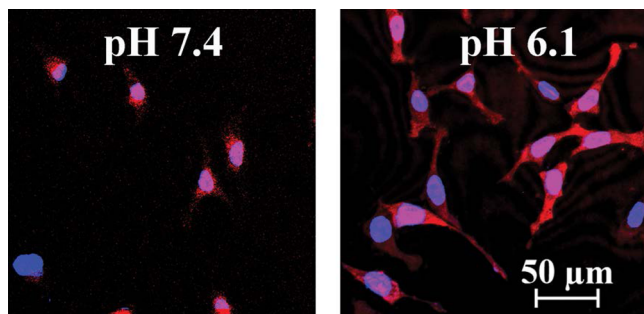


**Figure 7.** HeLa cells were treated with 1  $\mu$ M pHLIP-T-T construct for 20 min followed by 3X DPBS washing at pH 7.4 or 6.1. TAMRA fluorescence is in red, Hoechst fluorescence is in blue. The microscope image is taken at 24 h after the incubation. Rhodamine excitation is at 561 nm.

8a, b). The mean TAMRA-fluorescence intensities for pHLIP-FIRE constructs and for pHLIP-T are shown (Figure 8c), and their numeric values are given in Supporting Information Table 2. Strong tumor targeting was observed in each case, with very little off-target labeling detected in muscle, heart, spleen, and lungs. The fluorescence intensity was the highest in tumors labeled with pHLIP-T-Q and was the lowest in muscle for the pHLIP-T-T construct. Also, we observed an elevated uptake of the pHLIP-FIRE constructs in liver and kidneys compared to pHLIP-T.

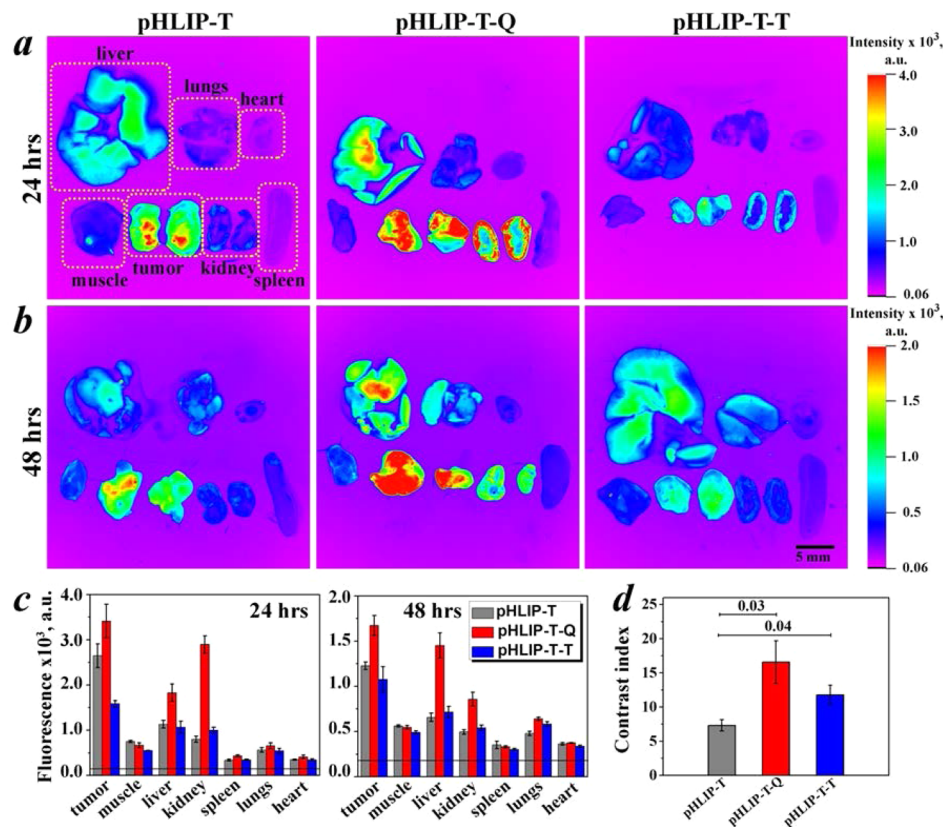


**Figure 8.** Biodistribution and contrast index of pHLIP-T-T, pHLIP-T-Q, and pHLIP-T. Fluorescent image of organs collected at 24 h (a) and 48 h (b) time after intravenous (IV) injection of constructs. (c) Mean fluorescence values of tumor and organs are shown for pHLIP-T (gray bars), pHLIP-T-Q (red bars), and pHLIP-T-T (blue bars) at 24 and 48 h after injection. The horizontal black line on the distribution panels indicates the level of instrument background fluorescence. The numeric values are presented in Supporting Information Table 2. (d) Contrast indices for all constructs at 24 h time intervals: pHLIP-T (gray bar), pHLIP-T-Q (red bar), pHLIP-T-T (blue bar). Error bars, standard error (SE) ( $n = 5$  mice). *p*-values for pHLIP-T-Q and pHLIP-T-T are shown on the graph.

To quantify improvement in tumor discrimination using the pHLIP-FIRE constructs as a result of the lower background, we compared the fluorescence intensities of tumors and non-targeted muscle tissues and calculated contrast index (CI), defined as the corrected tumor to background ratio:

$$CI = \frac{Fl_{tumor} - Fl_{auto}}{Fl_{norm} - Fl_{auto}}$$

where  $Fl_{tumor}$ ,  $Fl_{norm}$ , and  $Fl_{auto}$  are the mean fluorescence intensities of tumors, skeletal muscle, and the autofluorescence background signal from corresponding tissues in an untreated mouse, respectively.

The contrast index was substantially greater for the pHLIP-FIRE constructs than the unquenched pHLIP-T. After 24 h, the mean contrast indices were 11.7, 16.6, and 7.3 for pHLIP-T-T, pHLIP-T-Q, and pHLIP-T, respectively (Figure 8d). Thus, we achieved over 2-fold improvement in contrast using pHLIP-T-Q compared with the unquenched fluorescent probe, pHLIP-T. Because the pHLIP-FIRE signal in the muscle is close to zero after 48 h, we could not use CI as a parameter for quantitative measurement of the contrast. Division by a close-to-zero value results in high deviation in the mean value, which leads to statistically weak representation. However, we can calculate the ratio of average signals in tumor and muscle. These parameters show similar values at both 48 and 24 h time points. From this we conclude at least the same contrast at 48 h as at 24 h.

Here, we report a new tool, pHLIP-FIRE, for improved tumor to muscle contrast, and use it to demonstrate pHLIP delivery into tumor cells using systemic administration *in vivo*. Our strategy is similar to the “molecular beacon”, where a fluorophore-quencher pair is used to detect nucleic acid hybridization.<sup>26,27</sup> In each system, fluorescence quenching can be achieved by the close proximity of either two fluorophores (homo-quenching and H-dimer formation as in the case of pHLIP-T-T) or of a fluorophore–quencher pair (hetero-quenching as in the case of pHLIP-T-Q). Our approach is based on targeting of a quenched fluorescent pHLIP-FIRE construct to acidic tumors and activation of the fluorescence by translocating the cargo dye into cells, where the reducing power of the cytosol triggers the enhanced fluorescence. Testing the pH dependent interaction of pHLIP-FIRE with POPC membranes and with cultured cells demonstrated pHLIP-like pH dependent properties and fluorescence dequenching. When incubated with cells, the constructs showed 8- to 16-fold increase in fluorescence with a time course of dequenching on the order of 1–2 days. These background experiments set the stage for use *in vivo*.

Experiments using IV administration in mice resulted in the selective delivery and activation of the pHLIP-FIREs in tumors. Biodistribution studies of pHLIP-FIREs showed the highest accumulation in tumor sites. Slightly elevated levels of pHLIP-FIRE constructs were seen in liver and kidneys compared with the control fluorescent pHLIP construct with a single TAMRA. The activation of pHLIP-FIRE in kidneys was expected, since

the kidney is acidic, and labeling of kidneys by pHLIP has often been seen. The increase of fluorescence in liver most probably indicates a difference in the biodistribution of pHLIP-FIREs compared to pHLIP-T. Because pHLIP-FIRE constructs contain two nonpolar molecules (2 TAMRA or TAMRA plus QSY9), the increased overall hydrophobicity may facilitate liver uptake. Also, liver has the highest concentration of glutathione in the body, which may lead to a higher rate of dequenching.<sup>22</sup> In contrast with the cell-free and cellular dequenching results, pHLIP-T-T showed lower signal intensity compared to pHLIP-T-Q and pHLIP-T *in vivo*, which we think is most probably related to the difference in pharmacokinetics of the construct and the clearance time. Future designs may explore ways to reduce or avoid these problems by enhancing the polarity of pHLIP-FIRE, for example by adding polar groups to the pHLIP moiety or choosing more polar fluorophores/quenchers. Also, use of fluorescent dyes absorbing and emitting light at longer wavelengths than TAMRA will ensure better tissue penetration of light. However, we are mostly concerned with proof of principle in the present study, and the most important point is that a significant improvement in tumor-to-background ratio was achieved. A doubling of the contrast index for pHLIP-FIREs over nonquenched pHLIP-targeted imaging probes was observed, which allows better discrimination between healthy tissues and tumors, and points the way for further improvements.

The pHLIP-FIRE system has potential applications in fluorescence-guided surgery and may also have promise as a tool in cancer diagnosis. Not only have we improved the labeling contrast, but we have also shown targeted delivery of a model cargo (TAMRA or QSY9) into tumor cells *in vivo*, encouraging the further development of pHLIP for therapeutic applications in drug delivery.

## METHODS

**Chemical Syntheses of pHLIP-Constructs.** Detailed accounts of the chemical syntheses and characterizations of pHLIP-T, pHLIP-T-T, and pHLIP-T-Q constructs are provided in the Supporting Information. The control pHLIP-T construct was synthesized by reacting the pHLIP-Cys peptide (AAEQNPIYWA-RYADWLF-TTPLLDDLALLVDADEGTC) with tetramethyl-rhodamine, 6-maleimide. The pHLIP-FIRE constructs, pHLIP-T-T and pHLIP-T-Q, were synthesized from the pHLIP-KC peptide (AAEQNPIYWA-RYADWLFTTP-LLLDLALLV-DADEGTKCG). To produce pHLIP-T-T, first the C-terminal Cys side chain of pHLIP-KC is derivatized as an aminoethyl disulfide. Subsequent treatment with 5-TAMRA SE conjugates TAMRA to the primary amines of both the Lys side chain and the modified Cys sidechain. Synthesis of pHLIP-T-Q requires three steps: Reaction between QSY9 succinimidyl ester and S-(2-pyridylthio)cysteamine (step 1) provides a QSY9 derivative that is preactivated toward disulfide exchange with pHLIP-KC (step 2), which furnishes the C-terminal Cys side chain with the quencher QSY9 via a disulfide bond. Subsequent treatment of the intermediate with 5-TAMRA SE (step 3) conjugates TAMRA to the neighboring Lys sidechain via an amide bond. All intermediates and products were purified to greater than 90% purity using HPLC and their identities confirmed by molecular mass (via MALDI-TOF mass spectrometry to  $\pm 2$  Da of expected mass).

**Vesicle Preparation.** Large Unilamellar Vesicles (LUV) were prepared by extrusion. A required stock solution of POPC (1-palmitoyl-2-oleoyl-*sn*-glycero-3-phosphocholine, Avanti Polar Lipids, Inc.) in chloroform was concentrated under reduced pressure on a rotary evaporator and dried under vacuum overnight. The dried lipid film was rehydrated in 10 mM phosphate buffer at pH 8.0, vortexed, and repeatedly extruded (25 times) through a membrane with a pore size of 100 nm (Avanti Mini-Extruder).

**Chemical Dequenching and Circular Dichroism Measurements.** Fluorescence measurements were performed on an ISS Spectrofluorimeter. TAMRA was excited at 560 nm and fluorescence was recorded from 565 to 615 nm with the spectral widths of the excitation and the emission slits at 4 and 8 nm, respectively. Absorbance spectra were measured on Cary 100-Bio UV-visible spectrophotometer. The pHLIP-FIRE constructs were dissolved in 10 mM phosphate buffer (pH 8) at 1  $\mu$ M concentration. To confirm the quenching mechanism, L-glutathione (reduced form, Cayman Chemical Company) was added to the construct solution to achieve the desired final concentrations of the reducing agent (1, 3, or 10 mM). Before each experiment glutathione powder was flushed with nitrogen and then dissolved in pH 8.0 phosphate buffer. Circular dichroism (CD) was performed on JASCO J-810 spectropolarimeter. Spectra were recorded at 25 °C using a 2 mm cuvette. The solution of 2  $\mu$ M of pHLIP-FIRE in phosphate buffer (pH 8) was incubated with POPC vesicles at the molar lipid/peptide ratio of 200:1 and kept overnight. The pH of the samples was changed with small amounts of concentrated HCl acid.

**Cell Culture.** Human cervix adenocarcinoma (HeLa) and human lung carcinoma (A549) cells were obtained from the American Type Culture Collection (ATCC). An African green monkey fibroblast-like cells, COS-7, were a kind gift from Maureen Gilmore-Hebert and David F. Stern (Yale). The HeLa and COS-7 cells were cultured in DMEM supplemented with 4.5 g/L D-glucose, 10% FBS (Fetal Bovine Serum) (Gibco), and 1% penicillin. A549 cells were cultured in DMEM at pH 6.2 for several weeks to adjust the cells to a low pH environment. All the cells were grown in an incubator (Revco Elite II, Thermo Fisher Scientific) under humidified atmosphere of air and 5% CO<sub>2</sub> at 37 °C.

**Fluorescence Dequenching Experiments with Cells.** Cells were seeded in a UV sterilized 96-well collagen coated plate (Thermo Scientific) at a density of 5000 cells per well, and then grown close to 100% confluence level. Then, the cells were treated with 100  $\mu$ L of 1  $\mu$ M of a pHLIP fluorescent construct in Dulbecco's Phosphate Buffer Saline (DPBS, supplied with Ca<sup>2+</sup> and Mg<sup>2+</sup>) at pH 7.2 or pH 6.1. Incubation was done at RT (22–25 °C) under normal atmosphere in the biosafety cabinet. After 20 min the solution was removed and the cells were washed 3 times with pH 7.2 or 6.1 DPBS, and finally pH 7.2 or 6.1 DMEM was added to the cells. The pH 7.4 DMEM (no phenol red) is supplemented with 20 mM HEPES, whereas the pH 6.1 DMEM (no phenol red) is supplemented with 20 mM HEPES and 20 mM MES. Fluorescence was measured in a Berthold Tristar LB 941 plate reader with 535 nm excitation and 590 nm emission filters, respectively. Results obtained from five wells were averaged for each condition. The data points were fitted using a single exponential function with a sloped asymptotic line  $y = A \times \exp(-kt) + bx + y_0$ , where  $k$  is the rate constant,  $y$  is the normalized fluorescence intensity, and  $b$  is the linear component of the fluorescence signal. Cell viability was determined by adding a small aliquot of cell titer 96 Aqueous One solution cell proliferation MTS assay (Promega), with absorbance measured using a 490 nm filter over time. After the experiment, the pH of the DMEM was checked and it was found to increase no more than 0.3 pH unit (most likely due to the bicarbonate content in the DMEM buffer reacting with MES and/or HEPES acid).

**Confocal Microscopy.** HeLa cells were grown in glass bottom dishes (Electron Microscopy Science), and live cell confocal microscopy was performed on Zeiss LSM 510 NLO META using a 20 $\times$  objective. Incubation times and construct concentrations are the same as described for plate reader assays. The images were taken after 24 h of incubation with the construct. The cells were incubated with 4  $\mu$ g/mL Hoechst (Life Technologies) 30 min before imaging.

**Mouse Experiments.** BALB/c female mice ranging in age from 5 to 6 weeks were obtained from Harlan Laboratories (Indianapolis, IN). Mouse tumors were established by subcutaneous injection of 4T1 cells ( $8 \times 10^5$  cells/0.1 mL/flank) in the right flank of each mouse. When tumors reached 5–6 mm in diameter, tail vein injections of 150  $\mu$ L of 25  $\mu$ M of pHLIP-T-Q (5 mice), pHLIP-T-T (5 mice), or pHLIP-T (4 mice) were performed. Animals were euthanized at 24 or 48 h postinjections, and necropsy was performed immediately after

euthanization. Tumors and major organs were collected for imaging on a FX Kodak *in vivo* image station. Fluorescence intensity was obtained via analysis of images by using Kodak software. The tumor/background ratio was calculated according to the equation:

$$CI = \frac{Fl_{tumor} - Fl_{auto}}{Fl_{norm} - Fl_{auto}}$$

where  $Fl_{tumor}$ ,  $Fl_{norm}$ , and  $Fl_{auto}$  are the mean fluorescence intensities of tumor, muscle, and autofluorescence signal of the same organ from untreated mice, respectively.

## ASSOCIATED CONTENT

### Supporting Information

Description of chemical syntheses; pHLIP-FIRE dequenching rate constants; numeric fluorescence values of each organ. This material is available free of charge via the Internet at <http://pubs.acs.org>.

## AUTHOR INFORMATION

### Corresponding Author

\*Phone: 203-432-5601. Fax: 203-432-6381. Email: donald.engelman@yale.edu.

### Author Contributions

D.M.E., A.G.K., M.A., Y.K.R., and O.A.A. designed the project and wrote the manuscript. A.G.K., M.A., and L.Y. performed the experiments and analyzed data. A.G.K., R.A., and A.M. performed animal experiments. M.A., R.L., and L.Y. synthesized the constructs.

### Notes

The authors declare no competing financial interest.

## ACKNOWLEDGMENTS

We thank J. Deacon for fruitful discussions and comments on the manuscript, as well as for suggesting the name of pHLIP-FIRE. This work was supported by National Institutes of Health (NIH) grants CA133890 to O.A.A., D.M.E., and Y.K.R.; GM073857 to D.M.E.; and by SUNY, Binghamton University (BU) Research Foundation start-up funds to M.A. and L.Y., a HHMI-BU undergraduate summer fellowship to R.L., and National Science Foundation (NSF) grant CHE-0922815 for the Regional NMR Facility (600 MHz Instrument) at SUNY-Binghamton.

## REFERENCES

- (1) Gioux, S., Lomnes, S. J., Choi, H. S., and Frangioni, J. V. (2010) Low-frequency wide-field fluorescence lifetime imaging using a high-power near-infrared light-emitting diode light source. *J. Biomed. Opt.* 15, 026005.
- (2) Orosco, R. K., Tsien, R. Y., and Nguyen, Q. T. (2013) Fluorescence imaging in surgery. *IEEE Rev. Biomed. Eng.* 6, 178–187.
- (3) Nguyen, Q. T., and Tsien, R. Y. (2013) Fluorescence-guided surgery with live molecular navigation—A new cutting edge. *Nat. Rev. Cancer* 13, 653–662.
- (4) Brooks, J. D. (2012) Translational genomics: The challenge of developing cancer biomarkers. *Genome Res.* 22, 183–187.
- (5) Weerakkody, D., Moshnikova, A., Thakur, M. S., Moshnikova, V., Daniels, J., Engelmann, D. M., Andreev, O. A., and Reshetnyak, Y. K. (2013) Family of pH (low) insertion peptides for tumor targeting. *Proc. Natl. Acad. Sci. U.S.A.* 110, 5834–5839.
- (6) Gerweck, L. E., and Seetharaman, K. (1996) Cellular pH gradient in tumor versus normal tissue: Potential exploitation for the treatment of cancer. *Cancer Res.* 56, 1194–1198.
- (7) Warburg, O. (1956) On the origin of cancer cells. *Science* 123, 309–314.
- (8) Zhang, X., Lin, Y., and Gillies, R. J. (2010) Tumor pH and its measurement. *J. Nucl. Med.* 51, 1167–1170.
- (9) Tannock, I. F., and Rotin, D. (1989) Acid pH in tumors and its potential for therapeutic exploitation. *Cancer Res.* 49, 4373–4384.
- (10) Estrella, V., Chen, T., Lloyd, M., Wojtkowiak, J., Cornell, H. H., Ibrahim-Hashim, A., Bailey, K., Balagurunathan, Y., Rothberg, J. M., Sloane, B. F., Johnson, J., Gatenby, R. A., and Gillies, R. J. (2013) Acidity generated by the tumor microenvironment drives local invasion. *Cancer Res.* 73, 1524–1535.
- (11) Chiche, J., Brahimi-Horn, M. C., and Pouyssegur, J. (2010) Tumor hypoxia induces a metabolic shift causing acidosis: A common feature in cancer. *J. Cell Mol. Med.* 14, 771–794.
- (12) Reshetnyak, Y. K., Andreev, O. A., Segala, M., Markin, V. S., and Engelmann, D. M. (2008) Energetics of peptide (pHLIP) binding to and folding across a lipid bilayer membrane. *Proc. Natl. Acad. Sci. U.S.A.* 105, 15340–15345.
- (13) Reshetnyak, Y. K., Segala, M., Andreev, O. A., and Engelmann, D. M. (2007) A monomeric membrane peptide that lives in three worlds: In solution, attached to, and inserted across lipid bilayers. *Biophys. J.* 93, 2363–2372.
- (14) Andreev, O. A., Dupuy, A. D., Segala, M., Sandugu, S., Serra, D. A., Chichester, C. O., Engelmann, D. M., and Reshetnyak, Y. K. (2007) Mechanism and uses of a membrane peptide that targets tumors and other acidic tissues *in vivo*. *Proc. Natl. Acad. Sci. U.S.A.* 104, 7893–7898.
- (15) Segala, J., Engelmann, D. M., Reshetnyak, Y. K., and Andreev, O. A. (2009) Accurate analysis of tumor margins using a fluorescent pH Low Insertion Peptide (pHLIP). *Int. J. Mol. Sci.* 10, 3478–3487.
- (16) Cruz-Monserrate, Z., Roland, C. L., Deng, D., Arumugam, T., Moshnikova, A., Andreev, O. A., Reshetnyak, Y. K., and Logsdon, C. D. (2014) Targeting pancreatic ductal adenocarcinoma acidic microenvironment. *Sci. Rep.* 4, 4410.
- (17) Vavere, A. L., Biddlecombe, G. B., Spees, W. M., Garbow, J. R., Wijesinghe, D., Andreev, O. A., Engelmann, D. M., Reshetnyak, Y. K., and Lewis, J. S. (2009) A novel technology for the imaging of acidic prostate tumors by positron emission tomography. *Cancer Res.* 69, 4510–4516.
- (18) Viola-Villegas, N. T., Carlin, S. D., Ackerstaff, E., Sevak, K. K., Divilov, V., Srganova, I., Kruchevsky, N., Anderson, M., Blasberg, R. G., Andreev, O. A., Engelmann, D. M., Koutcher, J. A., Reshetnyak, Y. K., and Lewis, J. S. (2014) Understanding the pharmacological properties of a metabolic PET tracer in prostate cancer. *Proc. Natl. Acad. Sci. U.S.A.* 111, 7254–7259.
- (19) Reshetnyak, Y. K., Andreev, O. A., Lehnert, U., and Engelmann, D. M. (2006) Translocation of molecules into cells by pH-dependent insertion of a transmembrane helix. *Proc. Natl. Acad. Sci. U.S.A.* 103, 6460–6465.
- (20) An, M., Wijesinghe, D., Andreev, O. A., Reshetnyak, Y. K., and Engelmann, D. M. (2010) pH-(low)-insertion-peptide (pHLIP) translocation of membrane impermeable phalloidin toxin inhibits cancer cell proliferation. *Proc. Natl. Acad. Sci. U.S.A.* 107, 20246–20250.
- (21) Moshnikova, A., Moshnikova, V., Andreev, O. A., and Reshetnyak, Y. K. (2013) Antiproliferative effect of pHLIP-amanitin. *Biochemistry* 52, 1171–1178.
- (22) Moron, M. S., Depierre, J. W., and Mannervik, B. (1979) Levels of glutathione, glutathione reductase and glutathione S-transferase activities in rat lung and liver. *Biochim. Biophys. Acta* 582, 67–78.
- (23) Ogawa, M., Kosaka, N., Choyke, P. L., and Kobayashi, H. (2009) H-type dimer formation of fluorophores: A mechanism for activatable, *in vivo* optical molecular imaging. *ACS Chem. Biol.* 4, 535–546.
- (24) Reshetnyak, Y. K., Yao, L., Zheng, S., Kuznetsov, S., Engelmann, D. M., and Andreev, O. A. (2011) Measuring tumor aggressiveness and targeting metastatic lesions with fluorescent pHLIP. *Mol. Imaging Biol.* 13, 1146–1156.
- (25) Andreev, O. A., Engelmann, D. M., and Reshetnyak, Y. K. (2010) pH-sensitive membrane peptides (pHLIPs) as a novel class of delivery agents. *Mol. Membr. Biol.* 27, 341–352.

- (26) Tyagi, S., and Kramer, F. R. (1996) Molecular beacons: probes that fluoresce upon hybridization. *Nat. Biotechnol.* 14, 303–308.
- (27) Johansson, M. K., Fidder, H., Dick, D., and Cook, R. M. (2002) Intramolecular dimers: A new strategy to fluorescence quenching in dual-labeled oligonucleotide probes. *J. Am. Chem. Soc.* 124, 6950–6956.